IEEE Access
Multidisciplinary | Rapid Review | Open Access Journal

Received December 26, 2020, accepted January 29, 2021, date of publication February 9, 2021, date of current version February 22, 2021.

Digital Object Identifier 10.1109/ACCESS.2021.3058312

A Novel Voice-Coil Actuated Mini Crawler for In-Pipe Application Employing Active Force Control With Iterative Learning Algorithm

YASER SABZEHMEIDANI[1], MUSA MAILAH[2], (Senior Member, IEEE), TANG H. HING[2], AND SHERIF I. ABDELMAKSOUD[2]

[1]RoboMed Oy, 00290 Helsinki, Finland
[2]School of Mechanical Engineering, Universiti Teknologi Malaysia (UTM), Johor Bahru 81310, Malaysia

Corresponding author: Sherif I. Abdelmaksoud (iasherif@graduate.utm.my)

ABSTRACT This study proposes the design and development of an in-pipe mini crawler (or robot) capable of performing its various tasks with the ability to reject undesired disturbances resulting from friction and viscosity, as it was modeled, simulated, and experimented using an iterative learning algorithm (ILA)-based active force control (AFC) strategy. The crawler motion was executed based on a rapid and successive push-pull action plus friction that causes the crawler to move in an earthworm-like manner using a linear voice-coil actuator (VCA). A novel self-adjusted mechanism was designed to ensure that the crawler remained concentric in the pipe as it slides along the inner surface of the pipe. A novel control strategy was also proposed consisting of the AFC-based controller cascaded with a proportional-integral-derivative (PID) controller to control the crawler movement and expel off the applied perturbations. An intelligent PD-type ILA was employed to automatically tune the AFC while online. For the validation part, a prototype was designed, developed, and later experimented with using the proposed technique for a given set of conditions. The system integration employed a hardware-in-the-loop (HIL) test configuration utilizing LabVIEW. Experimental results are in good agreement with the simulation counterpart, thereby indicating the practicality and feasibility of the control system in performing accurate and robust trajectory tracking. This shall serve as a good basis for designing more challenging tasks related to miniature crawling mechanism in-pipe applications.

INDEX TERMS Mini crawler, voice-coil actuator, in-pipe application, self-adjusted mechanism, active force control (AFC), iterative learning algorithm (ILA).

I. INTRODUCTION

Nowadays miniature mechanisms or sometimes generally described as mini/micro robots are widely used in a number of engineering applications such as high-precision manipulation systems, intelligent micro-transportation systems, support surgical operation, and micro-fabrication process. One of the critical tasks is an in-pipe application, in which the robots are expected to operate in unstructured environments because of their enhanced adaptability to operate effectively even under hostile or unreachable conditions that may involve radioactivity, electromagnetic field, high-temperature gradient, and other hazardous environments. For industrial setting, in-pipe mini crawlers (as they may be regarded as the most practical applications in the pipe) can be equipped with appropriate instruments or micro tools to perform various tasks such as in-pipe inspection, leak detection, cleaning, condition monitoring, and biomedical applications [1]–[7]. Often, this type of application is typically related to a number of complications like an unreachable target (due to size restriction) or exposure to hazardous operating conditions (e.g., poisonous gas and/or chemical). In-pipe mini crawlers should be designed to enable them to adapt themselves to the environments with pipe constraints by incorporating new or novel types of actuators and mechanisms to facilitate such application. Besides, new materials that may produce high performance while maintaining low weight and micro-movement capability are being normally utilized in the design and

The associate editor coordinating the review of this manuscript and approving it for publication was Chaitanya U. Kshirsagar.

development of the mechanical aspects of the mechanism, thereby extend the value-added features of the system.

Junhong *et al.* [8] proposed a novel bilateral self-locking mechanism for an inchworm micro-in-pipe robot crawler in which they provided a detailed description of the operating principle. The robot was effectively demonstrated to glide effectively in a straight line pipe. However, the design is deemed intricate and complex to produce the desired motion. Another design was proposed by Jiang *et al.* [9] in which a spiral driving system and cage structure was developed. The device was realized experimentally and manage to produce a relatively large traction force at a certain speed using a small DC motor. Liu *et al.* [10] developed a micro-robotic mechanism that is based on the resonant driving principle which simplifies the transmission mechanism. It was rigorously tested in a pipe line environment.

The component that is deemed to be an integral or most important part of any miniature robotic system is the actuator used to provide the desired movement in the pipe to perform a specific task. The choice of the physical actuator in transforming from rigid movement to flexible or elegant motion involving the use of suitable material, parts, and control scheme that can emulate certain biological movement similar to the real-world counterpart (e.g., mimicking movement behavior or locomotion of small animals like an earthworm, snail, etc.) seems to be a promising proposition. A number of concepts highlighting the different mechanisms for movements in the pipe that can be used for the in-pipe application have been proposed like earthworm model [11], [12], wheel-based system [13], operating in bent-pipe [14], and tube crawler [15]. Inside a pipe, there is a number of different constraints in which a crawler should be able to adapt itself to variation in the pipe diameter (along with the pipe length), an inclination of the pipe, presence of a fluidic medium in the pipe, or the internal pipe surface conditions (rough, smooth, and lubricated, etc.). There are various actuators used for in-pipe crawler applications that can be found in literature such as those using piezoelectric actuators [16]–[18], electromagnetic actuators [19], or shape memory alloy (SMA) actuators [20]–[23], and pneumatic actuators [17].

Wang *et al.* [24] performed an analytical and experimental study in order to evaluate the characteristic influence of different structures on motion performance for a magnetic-actuated screw jet microrobot (SJM). While Fu *et al.* [25] suggested a microbiotic system in the form of a magnetic capsule, consisting of a magnetically actuated micro robot with a screw jet mechanism, a driving system, and a positioning system. Kim *et al.* [21] also proposed a mini crawler for in-pipe application in which one of the actuators is regarded as an extensor, which elongates to provide the longitudinal motion while the other two actuators serve as clampers. The traction of the mechanism is produced by adhering to the surface wall and the extensor providing the longitudinal motion along the pipe. With only one SMA actuator and silicon bellow, this combination plays a role in producing the contraction and extension similar to an earthworm muscle movement, thereby results in system locomotion. For piezoelectric actuators, Liu *et al.* [18] presented a micro robot design that is driven by impulsive voltages caused by the deflections of the piezoelectric bimorphs which in turn generated translational locomotion. The designed mechanism is composed of two thin circular bimorph sheets and an inertial mass. Developing a multiple-segment peristaltic crawling robot that uses DC motors was done in [11]. The resulting crawler movement is also likened to an earthworm behavior and a comparative study on various locomotion patterns for in-pipe application is also presented in the article.

In this article, a new and novel in-pipe mini crawler based on a linear voice coil actuator (VCA) is proposed. The voice-coil actuators possess some benefits like versatile direct drive, hysteresis-free, non-commuted limited motion servo motors with linear control characteristics. This type of actuator is ideal for high frequency and pull-push applications. VCAs prove to be more promising and practical compared to other actuators because of their high power, more stiffness, rapid response, and good performance in suitable displacement resolution. A voice coil (consisting of a former, collar, and winding) is the coil of wire attached to the permanent magnet. It provides the motive force to the coil by the reaction of a magnetic field to the current passing through it. Thus, the main mini crawler in-pipe motion in this study is produced by the VCA and its mechanism which has some benefits like versatile direct drive, hysteresis-free, non-commuted limited motion servo motors with linear control characteristics.

One of the main desirable and typical properties of a mini crawler for the in-pipe application that should be considered is to assume that it operates at the center of the pipe. In addition, it is also common to consider the variation in pipe diameter along the length of pipe and that the crawler's main mass should always remain concentric throughout the pipe while it is in operation for a specific application. For this purpose, a robust and efficient control mechanism is necessary to ensure that the system performs desirably and to expectation. The active force control (AFC) scheme as initially proposed by Hewit and Burdess [26] was selected as the main controller for controlling the dynamics of the system. This controller has a great ability to reject the unwanted disturbances which may be created due to friction forces or fluid/gas viscosity in the pipe. To determine the essential controller parameter related to the mass moment of inertia of the mini crawler robot, an intelligent method in the form of an iterative learning algorithm (ILA) was embedded into the AFC-based configuration. The performance of the control scheme was evaluated through a rigorous simulation study and subsequently validated via an experimental work.

The rest of the article is organized as follows: Section 2 describes the operating principle and mathematical modeling under certain assumptions. The PID controller and suggested AFC technique with ILC implementation are presented in Section 3. Section 4 shows the simulation results based on specific prescribed operating conditions goes on to experimental set-up, practical results, and

discussion in Section 5. Finally, the paper's conclusion is presented in Section 6.

II. VOICE-COIL ACTUATED MINI CRAWLER

A mini crawler mechanism proposed in this study works by a series of fast repetitive, impulsive shocks generated by the voice-coil actuator (VCA) that in turn causes the crawler to gradually surge forward in the pipe with help of friction between the masses and the inner wall of the pipe. These shocks directly lead to a high-frequency reciprocative force on the masses at both ends of the voice coil actuator, i.e., located at the front and rear ends of the mini crawler.

A. OPERATING PRINCIPLE

Figure 1 shows a basic structure of the voice-coil actuated mini crawler mechanism.

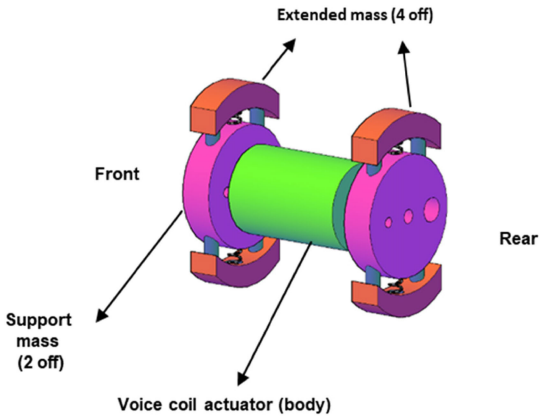

(a)

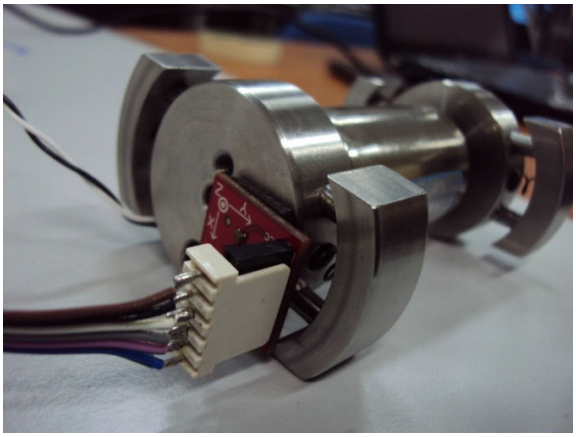

(b)

FIGURE 1. Self-adjustment mechanism of the mini crawler (a) 3D model (b) prototype.

The motion mechanism is based on friction and impulse force. The proposed in-pipe application mini crawler actuated by VCA has three components: the middle body (VCA itself), two support masses, and four extended masses that are connected to the front and rear of VCA. The dynamic characteristics of the mini crawler were derived by the formulation of a mathematical model, taking into account friction as the main disturbance element. A plan view of the VCA showing its operating principle in triggering the crawler reciprocative movement is shown in Figure 2.

The voice-coil actuated mini crawler essentially comprises the VCA itself as the main central body flanked by front and rear support and extended masses in the form of suitably sized segmented and protruding disks at both ends that are in partial contact with and concentrically touching the inner wall of the pipe. The materials for the support and extended masses (front and rear) were specifically selected to meet the following requirements, i.e., small, lightweight, simple construction, rigid, ease of fabrication, and integration to ensure that optimal and effective manipulation is possible inside the pipe. Thus, they were made of steel (ferrous material) and machined to size.

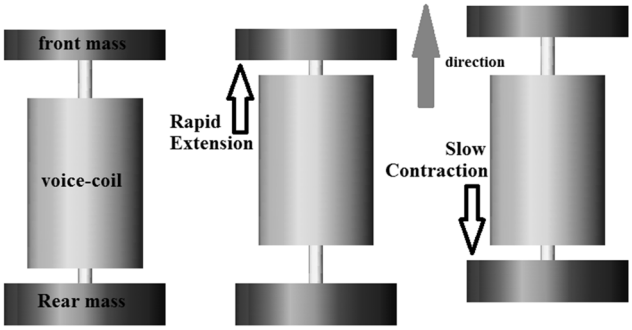

FIGURE 2. Operating principle of voice-coil actuated mini crawler (plan view).

The surging forward movement or traction of the mini crawler is realized when the system is switched on with the AFC-based control scheme triggered simultaneously. The design of the main mechanism (two masses) is based on the novel self-adjustment principle of the mini crawler about the center of the pipe by equipping the masses with a number of drilled holes (from the side towards the center of disks) and attaching two sets of support masses each containing a low stiffness spring located in special housing in the middle connected to mass support (with two guided rods) that allows the mini crawler to 'stick' comfortably to the inner surface or wall of the pipe. This configuration makes the protruding masses touch the inner surface of the pipe that conform concentrically with the inner pipe diameter and is particularly useful for a relatively long pipe that may be 'conical' or tapered along its length. Based on the action of the springs, the system can adjust itself with the variation of the pipe's inner diameter. Figure 3 shows the dimension of the mini crawler while Figure 4 depicts the free body diagram of the mini crawler's main mechanism.

The mini crawler is also equipped with a laser pointer for performing a specific application. The motion process of the mini crawler is described as follows:

a) The cycle starts with the actuator in rapid extension depending on the direction of movement of the mini crawler.

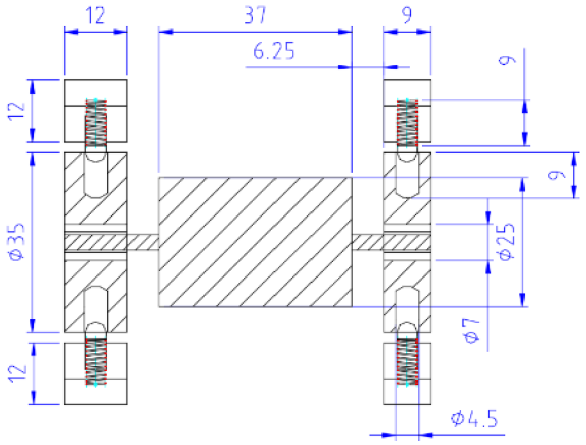

FIGURE 3. The dimension of mini crawler assembly (all in mm).

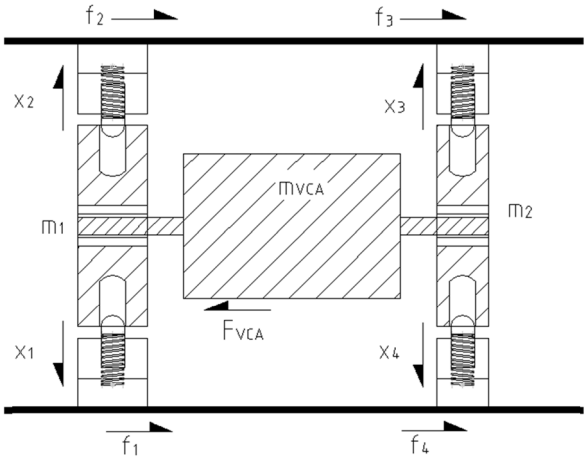

FIGURE 4. A free-body diagram of the mini crawler.

b) The VCA then returns back, also rapidly (but relatively slower than the extension phase) in the reverse direction, thereby creating a series of reciprocative impulses.
c) The continuous reciprocative impulse motion of the VCA with the friction effect between the extended masses and inner pipe surface plus inertia causes the mini crawler to slowly surge forward in the pipe.

The motion process showing the steps can be seen in Figure 2. The cycle is repeated continuously for the surging forward movement of the mini crawler in the direction of the extension. The motion amplitude of the actuator can be controlled by adjusting its step size. By repeating steps (a) to (c), it is possible to move the crawler for a long distance.

B. MATHEMATICAL MODELING

The basic operating principle of the VCA is ruled by the *Lorentz* force. The law of physics states that if a current-carrying conductor is placed in a magnetic field, a force will act upon it. The current I flow in the coil produces the VCA force, F_{VCA} is given by:

$$F_{\mathrm{VCA}} = K_{\mathrm{F}}(x)\,.I \tag{1}$$

where K_{F} is the force sensitivity of the actuator which depends on the position, x of the cylinder along the axis. From an electrical point of view, a model of VCA can be represented by the equivalent equation as follows:

$$E = RI + K_{\mathrm{B}}\left(\frac{dx}{dt}\right) + L\left(\frac{dI}{dt}\right) \tag{2}$$

where E is the external supply, R and L are the resistance and the inductance of the coil, respectively, and $K_{\mathrm{B}}\left(\frac{dx}{dt}\right)$ is the back electromotive force (BEMF) induced by the displacement of the voice-coil. The cylinder speed is $v = \left(\frac{dx}{dt}\right)$ and K_{B} is the BEMF constant. Equations (1) and (2) represent the two fundamental relationships of a linear VCA, and provide the basis for its dynamic behavior analysis. By applying *Newton*'s second law to the VCA, it is possible to describe the movement of the actuator and derive its dynamic model. m_{VCA} is assigned as the mass of the VCA and F_{EXT} is the external force along the x axis due to the mechanical load connected to it. The mini crawler is assumed to move along the horizontal axis and that there is no load on VCA so that F_{EXT} is zero. Thus, we have:

$$F_{\mathrm{VCA}} - F_{\mathrm{EXT}} = K_{\mathrm{F}}(x)\,.I = m_{\mathrm{VCA}}\left(\frac{d^2x}{dt^2}\right) \tag{3}$$

Based on *Newton* second law, for the whole mini crawler:

$$\sum F = ma = (m_1 + m_2 + m_{\mathrm{VCA}})\,a \tag{4}$$

where a is the total acceleration of mini crawler, m is the total mass of mini crawler, m_1 is front mass and m_2 is rear mass. The schematic diagram of the whole mechanism is shown in Figure 3 and based on the diagram:

$$\sum F = F_{\mathrm{VCA}} - F_{\mathrm{f}} \tag{5}$$

where F_{f} is the total friction forces (for dry surface) applied to mini crawler, noting that it is the sum of all individual friction forces at four locations and represented by f_1 to f_4 as shown in Figure 3. For the normal force and friction: mini crawler

$$F_{\mathrm{f}} = \mu_{\mathrm{K}} F_{\mathrm{N}} = \sum_{i=1}^{4} f_{\mathrm{i}} \tag{6}$$

where F_{N} is the total normal force applied from the inner surface of the pipe to the and μ_{k} is the coefficient of friction (between the inner surface of pipe and masses). It is expressed as:

$$F_{\mathrm{N}} = mg + F_{\mathrm{S}} = mg + k(\Delta x_1 + \Delta x_2 + \Delta x_3 + \Delta x_4) \tag{7}$$

where F_{S} is the total spring compression force against the inner surface of the pipe, k is the spring constant, and $\Delta x_{\mathrm{i}} = 1, 2, 3, 4$ represents each extended mass displacement (there is a total of four extended masses, namely, two each for the front and rear parts of the mini crawler mechanism as shown in Figure 3). By manipulating the above equations, we have:

$$K_{\mathrm{F}}(x)\,.I - \mu_{\mathrm{K}}(m_1 + m_2 + m_{\mathrm{VCA}})\,g + \mu_{\mathrm{K}}K(\Delta x_1 + \Delta x_2 + \Delta x_3 + \Delta x_4) = ma \tag{8}$$

Finally, the relationship between the acceleration of VCA and acceleration of the mini crawler is derived as:

$$m_{\mathrm{VCA}}\left(\frac{d^2x_{\mathrm{VCA}}}{dt^2}\right) - \mu_{\mathrm{K}}\left(m_1 + m_2 + m_{\mathrm{VCA}}\right)g + \mu_{\mathrm{K}}K\left(\Delta x_1 + \Delta x_2 + \Delta x_3 + \Delta x_4\right) = ma \quad (9)$$

III. AFC WITH ILA (AFCILA) SCHEME

The proposed controller was comprised of three main components, namely the conventional PID, AFC, and ILA. Each part was covered separately in the following sections.

A. PROPORTIONAL-INTEGRAL-DERIVATIVE (PID)

Since the PID control scheme is common, where its main equation is given as [27], [28]:

$$G_{\mathrm{c}}(\mathrm{s}) = K_{\mathrm{P}}e(\mathrm{s}) K_{\mathrm{I}}\frac{1}{\mathrm{s}}e(\mathrm{s}) + K_{\mathrm{D}}\mathrm{s}e(\mathrm{s}) \quad (10)$$

where K_{P}, K_{I}, and K_{D} are the proportional, integral, and derivative gains, respectively. While $e(\mathrm{s})$ is the error signal which is the difference between the reference and actual trajectories.

B. ACTIVE FORCE CONTROL (AFC)

The AFC method is a technique that relies on the appropriate estimation of the inertial or mass parameters of the dynamic system and the measurements of the acceleration and force signals induced by the system if a practical implementation is ever considered [26]. For theoretical simulation, it is normal to assume perfect modeling of the sensors and that the noises in the sensors are totally neglected. The underlying concept of AFC applied to a mini crawler is depicted in Figure 5.

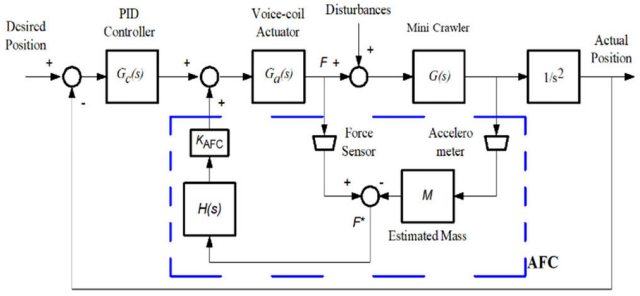

FIGURE 5. A block diagram of the proposed AFC-based scheme.

The estimated disturbance is obtained by considering the following expression:

$$F^* = \mathrm{F\text{-}M}a \quad (11)$$

The actuated force, F can be readily measured by means of a force sensor or indirectly through the use of current measurement (as in the case study) and the acceleration, using an accelerometer. The estimated mass, M may be obtained by assuming a perfect model, crude approximation, or intelligent methods [29], [30], noting that the ILA was explicitly used in the current work. F^* is then passed through a weighting function $H(s)$ to give the ultimate AFC signal command to be embedded with an outer control loop. This creates a controller that could provide excellent overall system performance provided that the measured and estimated parameters were appropriately acquired. The outer control loop can be a proportional-integral-derivative (PID) controller, resolved motion acceleration controller (RMAC), intelligent controller or others deemed suitable [29]. It is apparent that a suitable choice of $H(\mathrm{s})$ needs to be obtained that can cause the output to be made invariant with respect to the disturbances such that:

$$G_{\mathrm{a}}(\mathrm{s})H(\mathrm{s}) = 1 \quad (12)$$

A set of outer control loop control is applied to the above open-loop system, by first generating the world coordinate error vector, which would then be processed through a controller function, $G_{\mathrm{c}}(\mathrm{s})$, typically a classic PID controller that is used in the study. The controller mainly serves to complement the AFC loop to form a formidable and robust two DOF controller as rigorously implemented in many AFC-based schemes [26], [29], [30]. In another word, the AFC section should be cascaded with a conventional controller (notably PID controller) for its successful and effective implementation. The main computational burden in AFC is the multiplication of the estimated inertial parameter with the angular acceleration of the dynamic component before being fed into the AFC feed-forward loop. A useful point to note is that the constant K_{AFC} can effectively serve as a mode switch between the PID only scheme or PID method plus intelligent AFC method by simply setting the K_{AFC} to 0 or 1, respectively. On another note, it was established that AFC can accommodate a wide range of disturbances (known or unknown, linear or non-linear, measured or unmeasured, etc.), the largest of which is completely governed by the actuator bandwidth in terms of its power and size [26], [29], [30].

The notations used in Figure 5 are as follows:

$G(s)$:	Mini crawler transfer function
$G_{\mathrm{a}}(s)$:	Voice-coil actuator transfer function
$G_{\mathrm{c}}(s)$:	Outer loop PID controller transfer function
K_{AFC}:	AFC constant
$H(\mathrm{s})$:	Weighting function
F:	Applied force
F^*:	Estimated disturbance
M:	Estimated mass
a:	Linear acceleration

C. ITERATIVE LEARNING ALGORITHM (ILA)

The IL algorithm is an intelligent strategy through which the performance of a dynamical system (based on some error criterion) becomes better and better as time increases. Arimoto *et al.* [31] provided a sufficiently in-depth analysis of the convergence, stability, and robustness of the ILA which has been employed in this study. Figure 6 illustrates a schematic of the PD-type ILA.

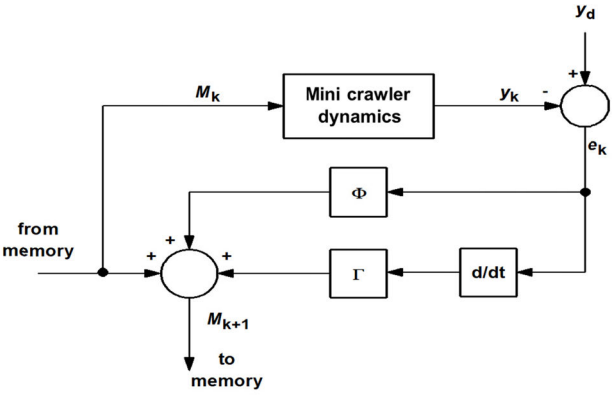

FIGURE 6. A PD-type ILA.

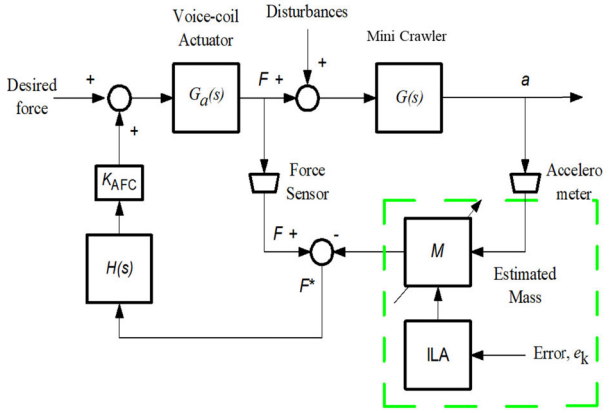

FIGURE 7. Block diagram of the AFCILA controller.

Based on Figure 5, the next value of the input signal, M_{k+1} can be expressed as:

$$M_{K+1} = M_K + \Gamma d/dt(e_K) + \phi e_K \tag{13}$$

where Φ and Γ are the proportional and derivative learning parameters, respectively and M is the estimated mass. The input signal (estimated mass) at k^{th} step M_k and the output signal y_k (actual trajectory) are stored in memory each time the system operates. The learning algorithm then evaluates the system performance error, e_k. Based on this error signal, the learning algorithm then computes a new input signal M_{k+1}, which is stored for use on the next iteration, i.e., the next time instant the system operates. The next input command is selected in such a way that it causes the performance error to be reduced on the next trial or iteration. One of the most important considerations in dealing with the IL is the convergence properties. An iterative method computes successive approximations such that the output of the system approaches an appropriate value as time increases. The learning process, however, is accomplished infinitely with the possibility of over-learning which could lead to instability of the system once it enters a 'danger zone'. Thus, a stopping criterion should be incorporated into the algorithm so that the system knows when to stop the learning process. Figure 7 shows a block diagram of the proposed intelligent AFC scheme that incorporates an ILA, to be known as AFCILA. Note that through ILA as in (13), the estimated mass (M) could be computed automatically and then passed to the AFC loop to trigger the compensation action. The fact that the algorithm is simple, makes the computation fast and almost readily implementable in real-time. An initial value of 0.25 kg was considered, and the best-computed value was obtained as 0.4 kg through the ILA. Thus, in this study, the reason for implementing the ILA is to compute the optimal value of the estimated inertia of the AFC strategy automatically, relatively fast, and on-line, as this can be seen to beneficially improve the system performance both analytically and experimentally. It is also useful to note that the time constant in the ILA has an effect on the computing speed of the estimated parameter; the smaller value tends to produce a slower response but of better accuracy and trajectory. A compromise was made to select its size so as to minimally affect the system performance and not jeopardizing its real-time implementation.

The PID, ILA, and AFC controller parameters used in the simulation study of AFCILA type are shown in Table 1. Note that the PID parameters were tuned using the *Ziegler-Nichols* method while the ILA learning constants heuristically tuned via a number of trial runs and that the values shown were considered the best or 'optimized' ones. The proposed mini crawler controllers were implemented considering two schemes; one without AFC and the other with an AFCILA controller. A number of input commands were introduced into the schemes as referenced trajectories. They are related to step, square, and saw-tooth wave functions. An applied disturbance is simulated in the form of a harmonic force, $H = \sin \omega t$ with a magnitude of 1 N, and a forcing frequency of 15 Hz was deliberately applied to the system to test the system robustness.

TABLE 1. Simulation Parameters for AFCILA.

Controller parameters	Values
***PID* controller:**	
Proportional gain (K_P)	45
Integral gain (K_I)	20
Derivative gain (K_D)	4
***ILA*:**	
Proportional learning parameter (Φ)	0.2
Derivative learning parameter (Γ)	0.2
***AFC* controller:**	
Percentage AFC	100%
Initial estimated mass (kg)	0.25

IV. SIMULATION RESULTS

The property of eliminating the effect of disturbance (disturbance rejection) is deemed to be the most important and desirable characteristic of a feedback controller. In this investigation, an intelligent proportional controller based on acceleration feedback was employed to reject the vibratory disturbances affecting the mini crawler. The responses to these inputs are shown in Figure 8. From the graphs, it can be seen that the PID controller is able to perform the trajectory tracking task satisfactorily by bringing the responses

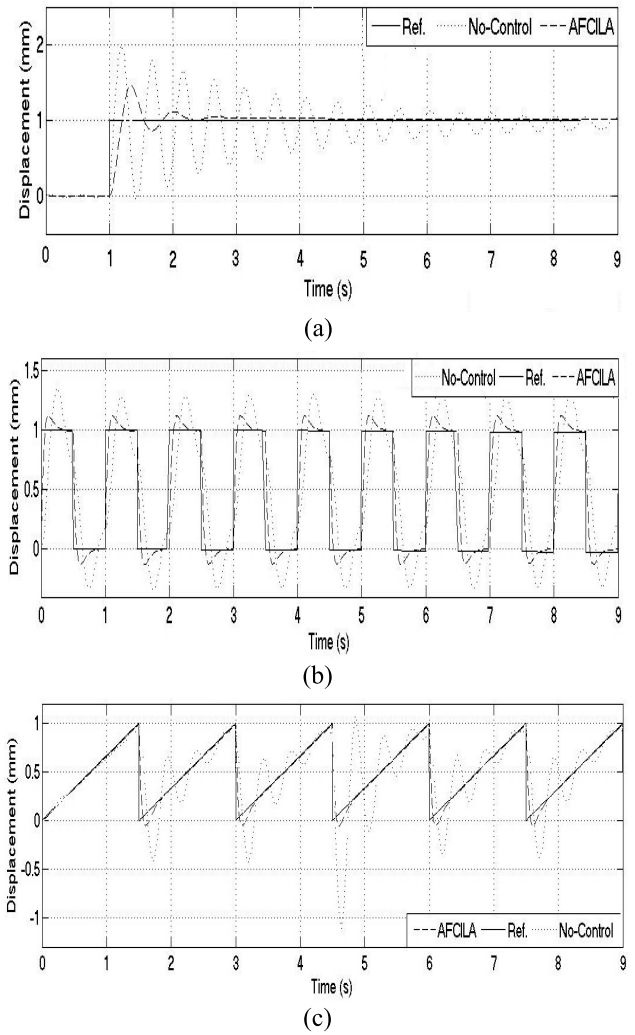

FIGURE 8. The system responses to various input conditions.

to converge to the reference positions but at the expense of relatively large tracking errors with substantial ripples or oscillation, largely due to the nature of the applied disturbance (vibratory). The AFCILA has a good ability to reject the disturbance but it takes some time to reach a stable point because of the learning time process. The intelligent control schemes show a good ability to reject the disturbance and make a robust movement.

V. EXPERIMENTAL WORKS AND DISCUSSION

The main specifications of the voice-coil actuated mini crawler are given in Table 2.

A schematic diagram of the experimental set-up showing the interlinking of all the main components is shown in Figure 9(a) while the developed physical system prototype or experimental rig can be seen in Figure 9(b). A data acquisition system (DAS) based on a *National Instrument* data acquisition (*NIDAQ*) card (*NI cDAQ-9174*) was carefully configured to provide the interfacing and control of the mini crawler through a LabVIEW graphic programming platform and the use of a PC-based controller (laptop).

TABLE 2. Main Specifications Related to the Voice-Coil Actuated Mini Crawler.

Parameter	Value	Parameter	Value
Stroke (mm)	5.1	μ_k	0.2
Moving mass (g)	24	Spring stiffness (N/m)	500
Total mass (g)	81	Peak force (N)	16
Resistance (ohm)	3.0	Front mass (g)	86
Inductance (mH)	0.7	Rear mass (g)	60

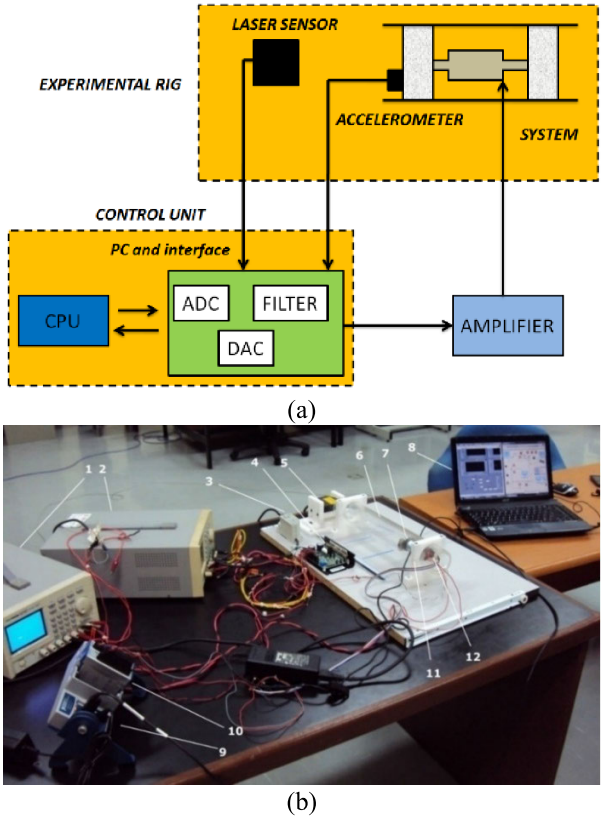

FIGURE 9. The experimental set-up: (a) schematic (b) a view of the physical mini crawler system.

1.DC power supply for the amplifier	7. VCA actuated mini crawler
2.DC Power supply	8. Laptop
3. Laser sensor controller board	9. *NI cDAQ-9174* card
4. VCA amplifier	10. I/O module
5. Laser displacement sensor head	11. Pipe holder
6. Perspex pipe	12. Accelerometer (*ADXL335*)

The input/output (I/O) devices related to the sensors (accelerometer and laser displacement sensor) and actuator (VCA) with their respective power supply units and driver were accordingly connected to the I/O module, *NIDAQ* card, and laptop. The accelerometer (*ADXL335*) and laser sensor have been appropriately calibrated prior to using it while for the force sensor, an indirect measurement was readily effected using a current 'sensor' through a simple electronic

circuitry, the measurement of which was then multiplied with the force sensitivity, K_F to yield the force as expressed in (1). Note that these measurements typically do not demand high accuracy for AFC application to affect its performance due to its robustness feature, implying that noises from the sensors could be well tolerated [26], [29], [30]. The main AFC equation in (11) thereby computes the estimated disturbance ($F*$) based on the measured force (F) and acceleration (a) and estimated mass (M).

The system integration constitutes a hardware-in-the-loop (HIL) test configuration that enables the real-time implementation of the proposed scheme. The programming part includes the control algorithm (AFCILA). The VCA used is of type *NCC05-11-011-1X* with a force sensitivity of 5.2 N/A and was operated using its driver (a linear current amplifier (LCAM)) as well as a signal generator that supplies the required frequency pulses, noting that the VCA was operated using a 15 Hz signal and with a 3 V DC power supply. The masses, springs, and guidance rods were connected via screws to the VCA main body. The accelerometer and the laser pointer were attached to the front mass and other related tools and connectors are as described and depicted in Figure 9. The disturbance is deliberately applied to the whole system through an electro-magnet which is placed underneath the pipe as shown in Figure 10. This has a tendency to slow the mini crawler movement in the pipe, thereby producing a kind of braking force, noting that both the support and extended masses (front and rear) of the mini crawler are made of ferrous material. Based on the specifications of the selected magnetic solenoid, the disturbance load is measured to be around 1 N. The perspex pipe has the following dimensions: internal diameter, 50 mm; thickness, 5 mm; and length, 500 mm. The operating conditions were set as follows:

- Steel support masses with ratio: $m_2/m_1 = 0.71$
- Supply voltage: $V = 3$ V
- Forcing frequency: $f = 15$ Hz

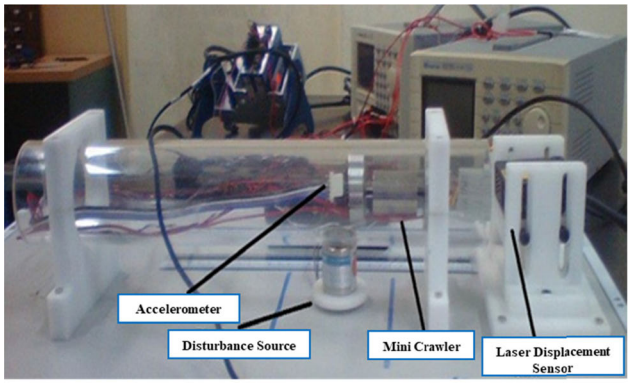

FIGURE 10. A close-up view of the in-pipe mini crawler with its instrumentation.

When the system was operated (switched on) based on the given settings, the mini crawler was seen able to move continuously along the inner surface of the pipe through the reciprocative action of the voice-coil actuated mechanism and the controller. The rapid push-pull effect creates an audible repetitive sound as the crawler moves by sliding along the inner surface of the pipe. The effective robot movement and its performance can be clearly seen by observing the characteristics pertaining to the crawler acceleration and error displacement as shown in Figures 11 and 12. The former figure shows the acceleration profile of the mini crawler in both uncontrolled and controlled modes. The controlled scheme shows a more systematic and well-produced trend as depicted in Figure 11(b) in comparison to the uncontrolled counterpart that contains some unnecessary sections and shorter operating periods as depicted in Figure 11(a). This implies that the crawler controlled movement with reference to the reciprocative action is more even, uniform, and regulated. Note that the mini crawler surge movement is the result of relatively rapid extension (pushing) of the VCA mechanism and relative slow pulling consequence in the opposite direction plus friction.

In the study, the crawler was allowed to move for approximately 2.5 cm in the pipe. It is possible to evaluate the capability of AFCILA to reject the unwanted disturbances applied to the voice-coil actuated mini crawler from observing the trend in Figure 12 that shows the displacement error with respect to the mini crawler movement. It is evident that Figure 12(b) shows a much-reduced displacement error profile, thereby signifying the robustness of the control scheme. In other words, it also implies that the system is able to overcome the disturbance in the form of the introduced braking force

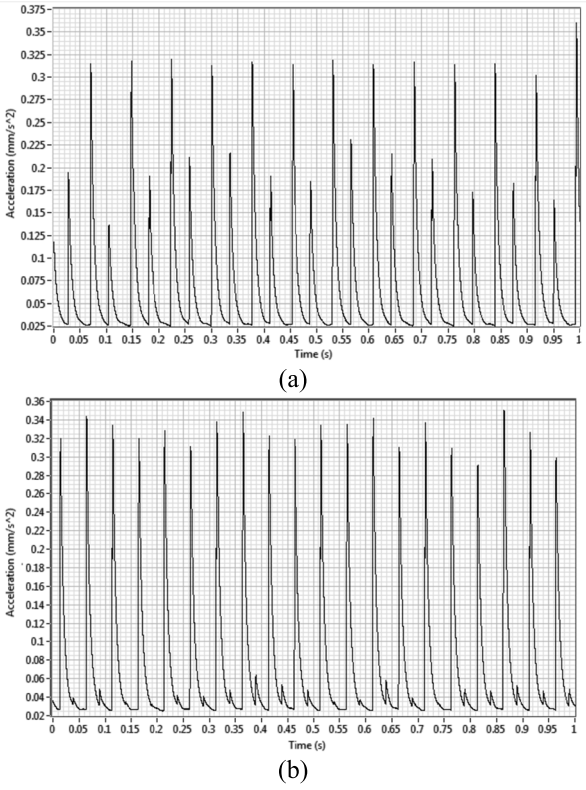

FIGURE 11. Mini crawler acceleration (a) without control (b) with AFCILA.

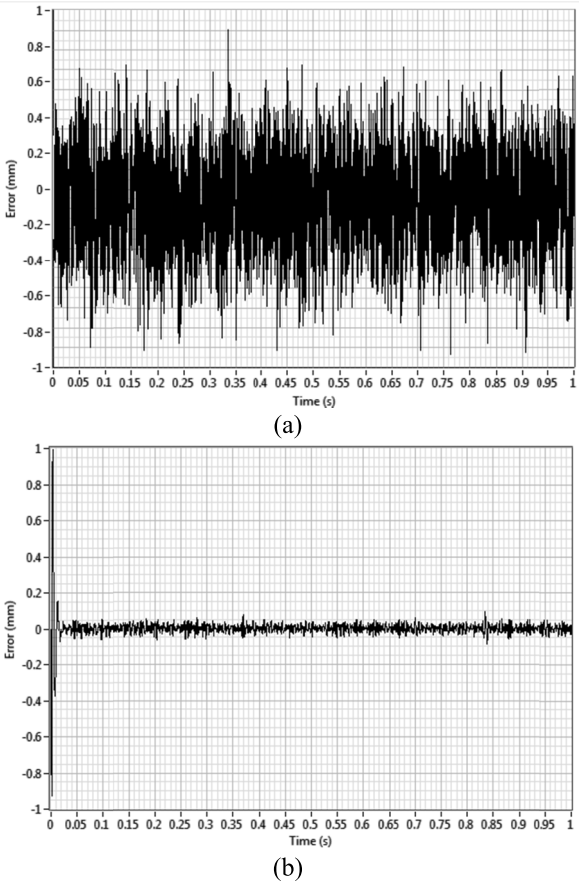

FIGURE 12. Displacement error (a) without control (b) with AFCILA.

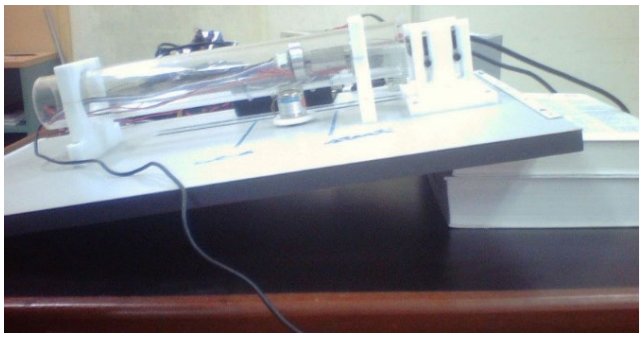

FIGURE 13. Mini crawler moves in an inclined pipe.

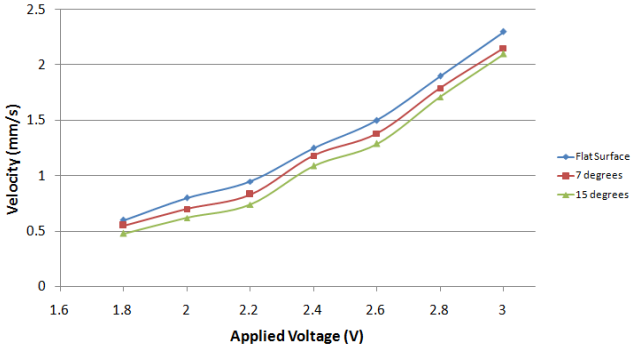

FIGURE 14. In-pipe mini crawler movement on inclined surfaces.

effectively. It is also expected that other forms of disturbances might produce almost similar results provided the excitation force does not exceed the bandwidth of the actuator in the AFC-based schemes. For the VCA model used in the research, the maximum generated continuous force is 5 N. Thus, the device is designed to operate not to exceed 5 N. For safety measure and due to the limitation of the amplifier, the maximum allowable force is limited to 3.5 N to avoid undue failure and the problem of the VCA. This is more than sufficient for most loading and operating conditions of the mini crawler in the pipe.

Having shown the ability of the controller to provide stable and robust movement and also to verify the system performance in the pipe for a given setting, an experiment was conducted to observe its surging forward movement in an inclined pipe. The system was tested considering three pipe tilting conditions, namely, flat surface (0° inclination), 7° inclination, and 15° inclination. A view of an inclined condition of the set-up is shown in Figure 13.

Figure 14 shows the result related to the effect of inclination on mini crawler movement in the presence of the disturbance. It clearly indicates an upward trend in the velocity for all cases for the corresponding increase in the applied voltages. Also, the mini crawler movement in a flat (zero inclination) pipe provides the highest velocity while the largest inclination produces the lowest trend. This is logically due to the gravitational effect; as the mini crawler moves upward, it has to accommodate or compensate for the higher gravitational load. The maximum velocity for the given setting is about 2.3 mm/s from a starting velocity of about 0.5 mm/s. Note that the velocity of the mini crawler is slightly affected by the introduced disturbance (electro-magnet). It is also noticed that there is not much effect of the inclination on the mini crawler movement, i.e., all the curve profiles are quite close to each other. This may be due to the self-adjustment mechanism plus the control action that makes the operation more robust and stable.

From the experimentation, it can be deduced that a number of limitations related to the design prevail. It is quite obvious that the traction and speed of the mini crawler are fully dependent on the VCA actuator (its bandwidth) model and that audible noise produced by the movement is unavoidable due to its successive and rapid reciprocative action caused by the internal operation of VCA as the main actuator. In addition, in its current form, the device is deemed not suitable for negotiating sharp corners in bent pipes including the right-angle ones (for small pipe) unless the design is further modified and upgraded to adapt to the changes in its operating environment. As it is, the mini crawler has been effectively tested for a straight pipe even with inclination.

VI. CONCLUSION

A novel voice-coil actuated mini crawler for in-pipe application has been successfully designed and developed. The locomotion of the mini crawler was made possible through the continuous reciprocative push-pull action brought about by the VCA and friction. It is mathematically modeled, simulated, and later validated via experiments using an AFC-based with ILA (AFCILA) controller. This control strategy is employed to ensure an accurate and robust trajectory tracking of the robot system in the presence of the prescribed disturbance and operating environments. The parameters of this controller are effectively estimated using an iterative learning algorithm (ILA) to trigger the compensation action. Simulation results show the robustness and superior performance of the AFC-based scheme in tracking the prescribed trajectories compared to the other schemes. The experimental rig was developed based on a full mechatronic approach with the system integration employing the hardware-in-the-loop (HIL) test via LabVIEW graphic programming environment and suitable I/O interface. Both the simulation and experimental results show good agreement, clearly affirming the effectiveness of the proposed AFCILA scheme. Future work may include a rigorous study on the effects of other parametric changes and various loading and operating conditions, and study of bent and tapered tubes as well, which greatly and significantly increases the theoretical contribution.

REFERENCES

[1] A. Nayak and S. K. Pradhan, "Investigations of design issues related to in-pipe inspection robots," *Int. J. Emerg. Tech. Adv. Eng.*, vol. 4, no. 3, pp. 819–824, 2014.

[2] J. Qiao, J. Shang, and A. Goldenberg, "Development of inchworm in-pipe robot based on self-locking mechanism," *IEEE/ASME Trans. Mechatronics*, vol. 18, no. 2, pp. 799–806, Apr. 2013, doi: 10.1109/TMECH.2012.2184294.

[3] Y.-G. Kim, D.-H. Shin, J.-I. Moon, and J. An, "Design and implementation of an optimal in-pipe navigation mechanism for a steel pipe cleaning robot," in *Proc. 8th Int. Conf. Ubiquitous Robots Ambient Intell. (URAI)*, Incheon, South Korea, Nov. 2011, pp. 772–773, doi: 10.1109/URAI.2011.6146010.

[4] M. O. Tătar, D. Mândru, and V. S. Jisa, "Development of the microrobot for indoor pipeline," *Appl. Mech. Mater.*, vol. 658, pp. 724–729, Oct. 2014, doi: 10.4028/www.scientific.net/AMM.658.724.

[5] J. Guo, S. Guo, X. Wei, and Q. Gao, "A novel tele-operation controller for wireless micro robots in-pipe with hybrid motion," *Robot. Auton. Syst.*, vol. 76, pp. 68–79, Feb. 2016, doi: 10.1016/j.robot.2015.07.009.

[6] L. Liang, H. Peng, B. Chen, Y. Tang, S. Chen, and Y. Xu, "Performance analysis and parameter optimization of an inner spiral in-pipe robot," *Robotica*, vol. 34, no. 2, pp. 361–382, Feb. 2016, doi: 10.1017/S0263574714001507.

[7] S. Guo, X. Wei, J. Guo, W. Wei, Y. Ji, and Y. Wang, "Development of a symmetrical spiral wireless microrobot in pipe for biomedical applications," in *Proc. IEEE Int. Conf. Robot. Autom. (ICRA)*, Hong Kong, May 2014, pp. 4705–4710, doi: 10.1109/ICRA.2014.6907547.

[8] J. Yang, Y. Xue, J. Shang, and Z. Luo, "Research on a new bilateral self-locking mechanism for an inchworm micro in-pipe robot with large traction," *Int. J. Adv. Robotic Syst.*, vol. 11, no. 10, p. 174, Oct. 2014, doi: 10.5772/59309.

[9] T. Jiang, Z. Luo, and J. Shang, "A spiral actuated micro in-pipe robot for pipes diameter 15 mm," *Adv. Mater. Res.*, vol. 871, pp. 315–322, Dec. 2013, doi: 10.4028/www.scientific.net/AMR.871.315.

[10] L. Liu, J. Li, W. Li, and J. Qin, "Design and experiment of a micro in-pipe robot based on the resonance," *Harbin Gongcheng Daxue Xuebao/J. Harbin Eng. Univ.*, vol. 35, no. 8, pp. 1002–1007, Aug. 2014, doi: 10.3969/j.issn.1006-7043.201305066.

[11] T. Nakamura, T. Kato, T. Iwanaga, and Y. Muranaka, "Development of a peristaltic crawling robot based on earthworm locomotion," *J. Robot. Mechatronics*, vol. 18, no. 3, pp. 299–300, 2006, doi: 10.3182/20060912-3-DE-2911.00027.

[12] A. Yamashita, K. Matsui, R. Kawanishi, T. Kaneko, T. Murakami, H. Omori, T. Nakamura, and H. Asama, "Self-localization and 3-D model construction of pipe by earthworm robot equipped with omni-directional rangefinder," in *Proc. IEEE Int. Conf. Robot. Biomimetics*, Phuket, Thailand, Dec. 2011, pp. 1017–1023, doi: 10.1109/ROBIO.2011.6181421.

[13] N. S. Roslin, A. Anuar, M. F. A. Jalal, and K. S. M. Sahari, "A review: Hybrid locomotion of in-pipe inspection robot," *Procedia Eng.*, vol. 41, pp. 1456–1462, 2012, doi: 10.1016/j.proeng.2012.07.335.

[14] Q. Liu, T. Ren, and Y. Chen, "Characteristic analysis of a novel in-pipe driving robot," *Mechatronics*, vol. 23, no. 4, pp. 419–428, Jun. 2013, doi: 10.1016/j.mechatronics.2013.03.004.

[15] F. Pfeiffer and T. Rossman, "Control of tube crawler," in *Proc. 4th Int. Conf. Motion Vib. Control, Movic, Zurich*, 1998, pp. 889–894.

[16] C. H. Pan, S. S. Tzou, and R. Y. Shiu, "A novel wireless and mobile piezoelectric micro robot," in *Proc. IEEE Int. Conf. Mechatronics Autom. (ICMA)*, Xi'an, China, Aug. 2010, pp. 1158–1163, doi: 10.1109/ICMA.2010.5588196.

[17] Q. H. Lu, G. Z. Yan, G. Q. Ding, and D. T. Yan, "The study on a miniature piezoelectric medical robot system," *Chin. J. Med. Instrum.*, vol. 28, no. 1, pp. 7–10, 2004.

[18] P. Liu, J. Wen, and N. Sun, "An in-pipe micro robot actuated by piezoelectric bimorphs," *Chin. Sci. Bull.*, vol. 54, no. 12, pp. 2134–2142, Jun. 2009, doi: 10.1007/s11434-009-0257-5.

[19] J. Chen, Z. Li, and Z. Zhang, "Pipe inspection mobile robot system based on electromagnetic micromotor with 4 mm diameter," *Micronanoelectron. Tech.*, vols. 7–8, no. 7, pp. 570–572, 2003. [Online]. Available: http://caod.oriprobe.com/articles/6497359/Pipe_inspection_mobile_microrobot_system_based_on_electromagnetic_micr.htm, doi: 10.1117/12.483162.

[20] H. Yu, P. Ma, and C. Cao, "A novel in-pipe worming robot based on SMA," in *Proc. IEEE Int. Conf. Mechatronics Automat. (ICMA)*, Niagara Falls, ON, Canada, 2005, pp. 923–927, doi: 10.1109/ICMA.2005.1626675.

[21] B. Kim, M. G. Lee, Y. P. Lee, Y. Kim, and G. Lee, "An earthworm-like micro robot using shape memory alloy actuator," *Sens. Actuators A, Phys.*, vol. 125, no. 2, pp. 429–437, Jan. 2006, doi: 10.1016/j.sna.2005.05.004.

[22] M. Bodnicki and D. Kamiński, "In-pipe microrobot driven by SMA elements," in *Proc. 10th Int. Conf. Mechatronics*, Brno, Czech Republic, 2014, pp. 527–533, doi: 10.1007/978-3-319-02294-9_67.

[23] M. C. Carrozza, A. Arena, D. Accoto, A. Menciassi, and P. Dario, "A SMA-actuated miniature pressure regulator for a miniature robot for colonoscopy," *Sens. Actuators A, Phys.*, vol. 105, no. 2, pp. 119–131, Jul. 2003, doi: 10.1016/S0924-4247(03)00086-4.

[24] Z. Wang, S. Guo, Q. Fu, and J. Guo, "Characteristic evaluation of a magnetic-actuated microrobot in pipe with screw jet motion," *Microsyst. Technol.*, vol. 25, no. 2, pp. 719–727, Feb. 2019, doi: 10.1007/s00542-018-4000-5.

[25] Q. Fu, S. Zhang, S. Guo, and J. Guo1, "Performance evaluation of a magnetically actuated capsule microrobotic system for medical applications," *Micromachines*, vol. 9, no. 12, pp. 1–16, 2018, doi: 10.3390/mi9120641.

[26] J. R. Hewit and J. S. Burdess, "Fast dynamic decoupled control for robotics using active force control," *Mech. Mach. Theory*, vol. 16, no. 5, pp. 535–542, 1981, doi: 10.1016/0094-114X(81)90025-2.

[27] S. I. Abdelmaksoud, M. Mailah, and A. M. Abdallah, "Robust intelligent self-tuning active force control of a quadrotor with improved body jerk performance," *IEEE Access*, vol. 8, pp. 150037–150050, 2020, doi: 10.1109/ACCESS.2020.3015101.

[28] S. I. Abdelmaksoud, M. Mailah, and A. M. Abdallah, "Practical real-time implementation of a disturbance rejection control scheme for a twin-rotor helicopter system using intelligent active force control," *IEEE Access*, vol. 9, pp. 4886–4901, 2021, doi: 10.1109/ACCESS.2020.3046728.

[29] M. Mailah, "Intelligent active force control of a rigid robot arm using neural network and iterative learning algorithms," Ph.D. dissertation, Dept. Appl. Phys., Elect. Mech. Eng., Univ. Dundee, Dundee, U.K., 1998.

[30] G. Priyandoko, M. Mailah, and H. Jamaluddin, "Vehicle active suspension system using skyhook adaptive neuro active force control," *Mech. Syst. Signal Process.*, vol. 23, no. 3, pp. 855–868, Apr. 2009, doi: 10.1016/j.ymssp.2008.07.014.

[31] S. Arimoto, S. Kawamura, and F. Miyazaki, "Bettering operation of robots by learning," *J. Robotic Syst.*, vol. 1, no. 2, pp. 123–140, Summer 1984, doi: 10.1002/rob.4620010203.

YASER SABZEHMEIDANI was born in Babol, Iran, in 1983. He received the B.S. and M.S. degrees in mechanical engineering from the University of Mazandaran, Babol, in 2006 and 2008, respectively, and the Ph.D. degree from Universiti Teknologi Malaysia (UTM), in 2013. He is currently pursuing his career in medical robots at RoboMed Oy as the Managing Director. His research interests include mechatronics, AI supported control algorithms, CAD/CAM, robotics, and manufacturing.

MUSA MAILAH (Senior Member, IEEE) received the B.Eng. degree in mechanical engineering from Universiti Teknologi Malaysia (UTM), in 1988, and the M.Sc. degree in mechatronics and the Ph.D. degree in robot control and mechatronics from the University of Dundee, U.K., in 1992 and 1998, respectively. He is currently a Professor with the Faculty of Engineering, School of Mechanical Engineering, UTM, where he is also the Head of the Intelligent Control and Automation (iCA) Research Group. His research interests include intelligent systems, active force control of dynamical systems, robot control, mobile manipulator, applied mechatronics and industrial automation. He is a registered Chartered Engineer (C.Eng.), U.K.

TANG H. HING received the B.Eng. and M.Eng. degrees in mechanical engineering from Universiti Teknologi Malaysia (UTM), in 2002 and 2005, respectively, and the Ph.D. degree in electrical engineering (biomedical) from the University of New South Wales, Sydney, Australia. He is currently a Senior Lecturer with the Department of Applied Mechanics and Design, UTM. His research interests include the development of robotic device for gait rehabilitation, use of respiratory induced cardiovascular signal variations to monitor the fluid status in a mechanical ventilated end toxic shock rabbits, and application of machine learning algorithms (especially SVM) in clinical decision making or diagnosis and robotic motion planning and system control.

SHERIF I. ABDELMAKSOUD received the M.S. degree in aerospace engineering from the King Fahd University of Petroleum & Minerals (KFUPM), Saudi Arabia, in 2015. He is currently pursuing the Ph.D. degree with the School of Mechanical Engineering, Universiti Teknologi Malaysia (UTM), Malaysia. His research interests include dynamic systems modeling, active force control, active vibration control, intelligent control systems, and autonomous unmanned aerial vehicles (UAVs).